AD-A079 805 HUGHES RESEARCH LABS MALIBU CA F/G 20/6
BLUE/GREEN COUPLED WAVE FILTER STUDY.(U)
JAN 80 J F LOTSPEICH, D M HENDERSON N00014-79-C-0491

UNCLASSIFIED NL

1 OF 1
AD-
A079805

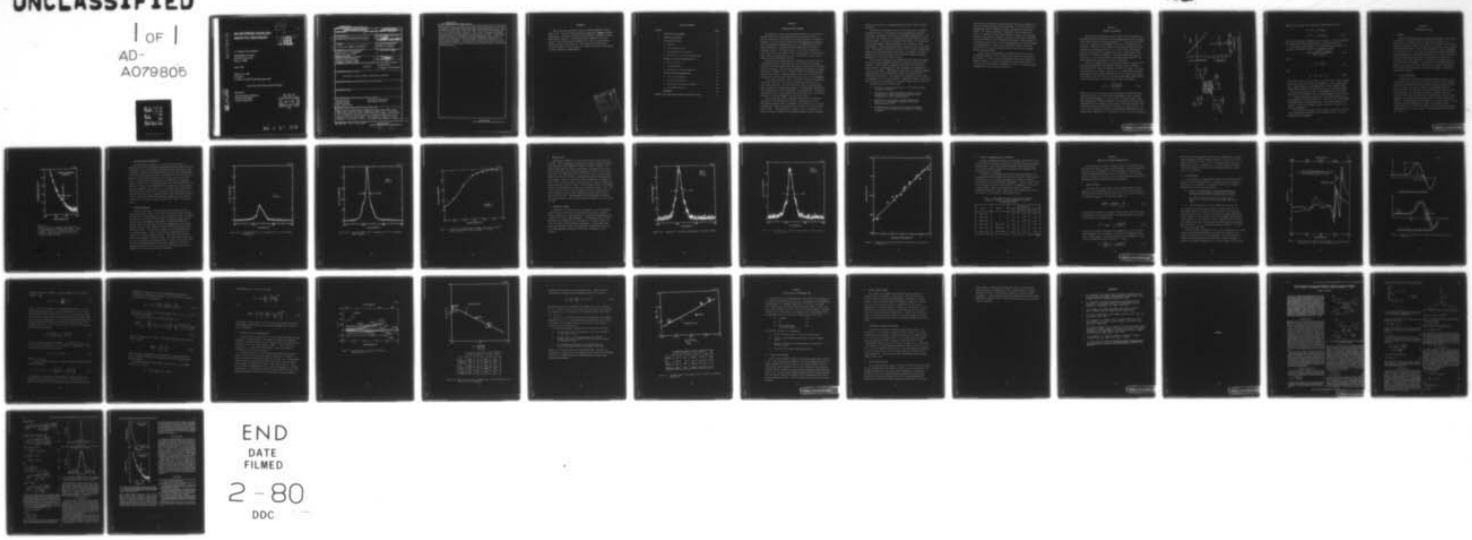

END
DATE
FILMED
2-80
DDC

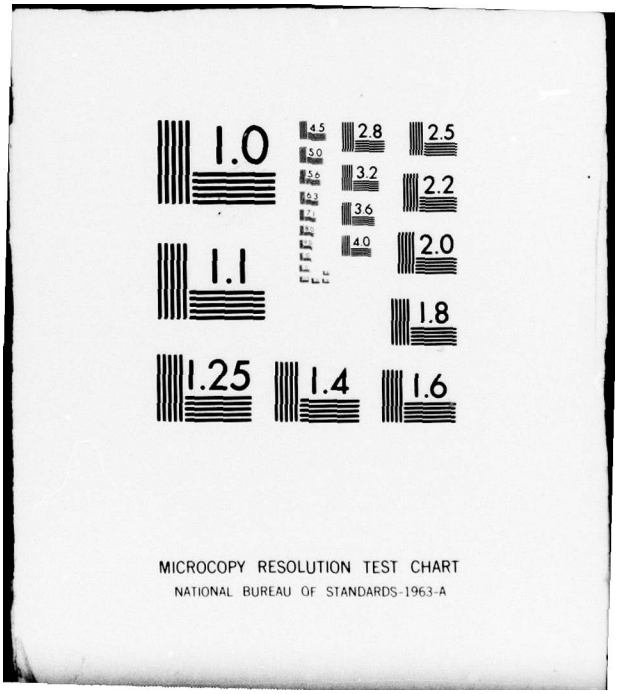

(12)

12

BLUE/GREEN COUPLED WAVE FILTER STUDY

LEVEL II

J.F. Lotspeich and D.M. Henderson

Hughes Research Laboratories
3011 Malibu Canyon Road
Malibu, CA 90265

January 1980

N00014-79-C-0491
Final Report
For period 1 June 1979 through 30 November 1979

Approved for public release; distribution unlimited.

Sponsored By

OFFICE OF NAVAL RESEARCH
Physical Sciences Division
Arlington, Virginia 22217

UNCLASSIFIED

SECURITY CLASSIFICATION OF THIS PAGE (When Data Entered)

REPORT DOCUMENTATION PAGE

READ INSTRUCTIONS BEFORE COMPLETING FORM

1. REPORT NUMBER

2. GOVT ACCESSION NO.

3. RECIPIENT'S CATALOG NUMBER

4. TITLE (and Subtitle)

BLUE/GREEN COUPLED WAVE FILTER STUDY.

5. TYPE OF REPORT & PERIOD COVERED

Final Report.
1 Jun [redacted] — 30 Nov [redacted] 79

6. PERFORMING ORG. REPORT NUMBER

7. AUTHOR(s)

J.F. Lotspeich [redacted] D.M. Henderson

8. CONTRACT OR GRANT NUMBER(s)

N00014-79-C-0491

9. PERFORMING ORGANIZATION NAME AND ADDRESS

Hughes Research Laboratories
3011 Malibu Canyon Road
Malibu, CA 90265

10. PROGRAM ELEMENT, PROJECT, TASK AREA & WORK UNIT NUMBERS

421

11. CONTROLLING OFFICE NAME AND ADDRESS

Office of Naval Research
Physical Sciences Division
Arlington, Virginia 22217

12. REPORT DATE

Jan [redacted] 80

13. NUMBER OF PAGES

50

14. MONITORING AGENCY NAME & ADDRESS (if different from Controlling Office)

12 4/2

15. SECURITY CLASS. (of this report)

UNCLASSIFIED

15a. DECLASSIFICATION DOWNGRADING SCHEDULE

16. DISTRIBUTION STATEMENT (of this Report)

Approved for public release; distribution unlimited.

17. DISTRIBUTION STATEMENT (of the abstract entered in Block 20, if different from Report)

18. SUPPLEMENTARY NOTES

19. KEY WORDS (Continue on reverse side if necessary and identify by block number)

Optical filter
Blue-green band
Narrow passband
Wide field of view
Iso-index characteristic
Electrooptic coupling

20. ABSTRACT (Continue on reverse side if necessary and identify by block number)

High-resolution measurements of $AgGaS_2$ iso-index electrooptic filter samples have confirmed earlier theoretical predictions. We observed a filter passband of less than 1.0 Å at 4970 Å in a sample 3 mm thick and have achieved electrooptic control of transmission efficiency up to a maximum of 60% with about 1000 V. These results translate to filter passbands of less than 0.3 Å in a 1-cm sample with comparable voltage → next page

DD FORM 1 JAN 73 1473 EDITION OF 1 NOV 65 IS OBSOLETE

UNCLASSIFIED

SECURITY CLASSIFICATION OF THIS PAGE (When Data Entered)

172 600

deg.

requirements and with negligible electric power dissipation. The filter response for off-normal light beams indicates an FOV capability in excess of 60° half-angle (f/0.3) with less than a 20% increase in passband over that of the narrow-field condition. Fine tuning of the pass wavelength by temperature variation showed a tuning rate of 0.25 Å/°C. Theoretical characterization of iso-index materials demonstrated that crystals with large nonresonant birefringence and small fundamental bandgap shifts yield narrow passbands. A useful figure of merit for predicting filter performance was derived. Potentially useful materials include the II-VI mixed crystal semiconductors (CdS-ZnO) and the mixed ternary chalcopyrites ($AgGaS_2^n$-$CuAlS_2^n$).

FOREWORD

This is the final technical report on Contract N00014-79-C-0491, Project 421. The work reported here was accomplished by Hughes Research Laboratories, a division of Hughes Aircraft Company, 3011 Malibu Canyon Road, Malibu, CA 90265. This research was accomplished during the period 1 June 1979 through 30 November 1979. The U.S. Navy program monitor was M.B. White, Code 421. This document was submitted on 31 January 1980; its authors were J.F. Lotspeich, principal investigator, and D.M. Henderson, program manager.

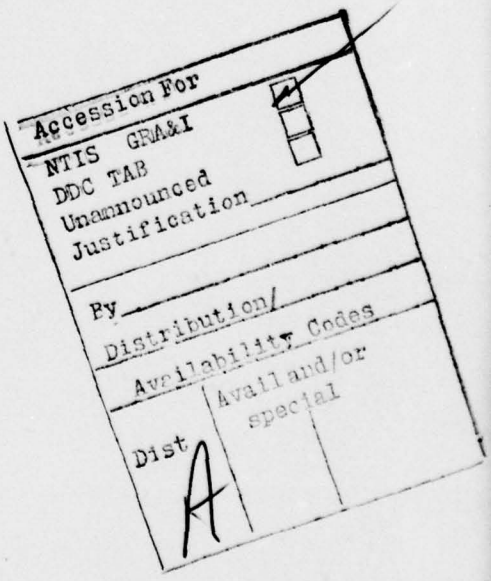

TABLE OF CONTENTS

SECTION 1

INTRODUCTION AND SUMMARY

The ability of light in the blue-green portion of the spectrum to penetrate sea water to operational depths has created interest in optical communications from space and airborne platforms to submerged terminals. Of the various blue/green optical communications programs, the most demanding requirements are set by the OPSATCOM scenario, in which information is transmitted from a synchronous satellite to a submarine at depth. The link requires a filter with a bandwidth of $\sim$0.1 Å and field of view (FOV) of ±45° ($\sim$f/0.5 optics). These requirements cannot be simultaneously met with conventional filters (such as dielectric layer interference filters).

Although optical communications to submerged stations has been of considerable interest to the Navy since the invention of the laser, projected systems performance has been severely limited by the available receiver technology. Several factors complicate the problem in a marine environment, including loss of coherence caused by multiple scattering, wavefront distortion in passing through the air-water interface, and uncertainty in pointing that requires the target to be over illuminated.

The blue-green filters require a wide FOV to allow the transmitted laser light scattered by the air-sea interface and sea water to be efficiently collected. The filter must also have a very narrow passband to minimize the background sunlight. In conventional interference filter approaches, the two requirements are contradictory. Conventional interference filters include Fabry-Perot, dielectric layer interference, acoustooptic, and birefringent (Lyot and Solc) filters.

Since conventional filter techniques cannot meet the blue-green requirements, new approaches are needed. A modified Lyot filter developed by Lockheed, with a bandwidth of $\sim$1 Å, FOV of ±30°, and peak transmission of $\sim$40%, is projected to be the state of the art in blue/green filters. Narrowband atomic resonance filters, investigated by Lawrence Livermore Laboratory and McDonnell-Douglas, exhibit promising

features but operate at a fixed wavelength and have a limited FOV and efficiency.

The present work followed from an earlier Navy contract (N00014-78-C-0201) in 1978 to investigate new filter approaches to meet the challenging requirements of satellite-to-submarine communications. The study led to the concept of the iso-index coupled-wave filter in which polarized light is selectively coupled from the fast to the slow axes in certain birefringent crystals exhibiting a zero crossing in their birefringence. This zero-crossing point is referred to as the iso-index point. The calculated performance of this class of filters showed great promise for meeting blue/green requirements. For example, a filter of $AgGaS_2$, which has its iso-index point at 4970 Å, showed a calculated bandwidth of $\sim$0.2 Å over a full 2π sr FOV.

On the present program, we have fabricated test devices and demonstrated the narrow-bandwidth and wide-FOV properties offered by this technique. Specifically, our $AgGaS_2$ filters with 3-mm interaction length showed a 0.94-Å bandwidth. This translates to a bandwidth of 0.3 Å in a 1-cm sample. Measurements showed that the bandwidth degraded insignificantly with extreme off-axis light, as expected from our theoretical calculations. The largest offset measured was ±60°, which corresponds to an f/0.3 optical system. Temperature tuning of the filter above 4970 Å was demonstrated with a measured tuning rate of $\sim$0.25 Å/°C.

Proposed future work includes the:

- Extension of active filter area to 1 cm^2 from the present few square millimeters.
- Improvement of crystal annealing techniques to remove residual strain, which is presently limiting filter transmission to $\sim$60% (polarized light).
- Evaluation of an alternate coupling mechanism that would use an intentionally directed strain rather than an electric field.
- Determination of the out-of-band rejection efficiency of the filter and techniques to increase the rejection if needed.

The successful completion of these tasks will allow us to demonstrate a filter of practical dimensions with bandwidth <0.3 Å, FOV >±45°, and transmission >40% for unpolarized light, operating in a range about 4970 Å. This filter wavelength is compatible with the HgBr laser, which is a candidate for the laser transmitter source. The iso-index approach could also be extended, if desired, to the shorter wavelength region near 4800 Å, where the Raman-shifted excimer lasers operate, by using mixed crystals, such as II-VI semiconductors or I-III-VI chalcopyrite semiconductors. Thus, future development should be viewed as applicable to the entire blue/green region, rather than to a single, limited wavelength range.

A brief technical background is presented in Section 2; a more detailed presentation of the iso-index filter concept is reserved for the appendix. Section 3 covers experimental results with laboratory samples of $AgGaS_2$. A theoretical analysis of the characteristics of iso-index filter materials is developed in Section 4. Conclusions and recommendations are presented in Section 5.

SECTION 2

TECHNICAL BACKGROUND

During our 1978 exploratory contract study of novel techniques for narrowband, wide-FOV filtering in the blue/green spectral band, a promising new kind of optical filter was designed.[1,2,3] This device is based on the zero crossing of birefringence that occurs in $AgGaS_2$ near its band edge. Coupling of light energy is induced between principal polarizations at the isotropic point by a dc electric field. When placed between crossed polarizers, $AgGaS_2$ thus acts as a narrow-band filter. The device is called, accordingly, an iso-index coupled-wave electro-optic filter. The unique features of this and related filters[4,5] are their simultaneous high selectivity and very wide FOV.

The filter configuration is illustrated in Figure 1, together with the wavelength-dependent birefringence of $AgGaS_2$ and the resultant theoretical filter transfer characteristic for a 1-cm sample. An alternative selection of crystal cut allows use of a transverse rather than longitudinal electric field. Applying an electric field $\mathscr{E}_1$ in a direction normal to the optic axis in a crystal such as $AgGaS_2$ ($\bar{4}2m$ symmetry) causes the optic axis to rotate through an angle α according to

$$\tan 2\alpha = \frac{2n_o^2 n_e^2 r_{41} \mathscr{E}_1}{n_o^2 - n_e^2} , \qquad (2.1)$$

where n_o and n_e are the ordinary and extraordinary refractive indices, respectively, and r_{41} is the relevant electrooptic tensor component. With finite birefringence, α is in practice a very small angle. Thus, light entering the crystal and having its polarization either parallel or perpendicular to the original optic axis will essentially maintain that direction through the crystal and be blocked by a crossed analyzer. At a particular wavelength λ_o where the birefringence disappears (in zero field), α goes abruptly to 45°, according to Eq. 2.1, and the field-induced

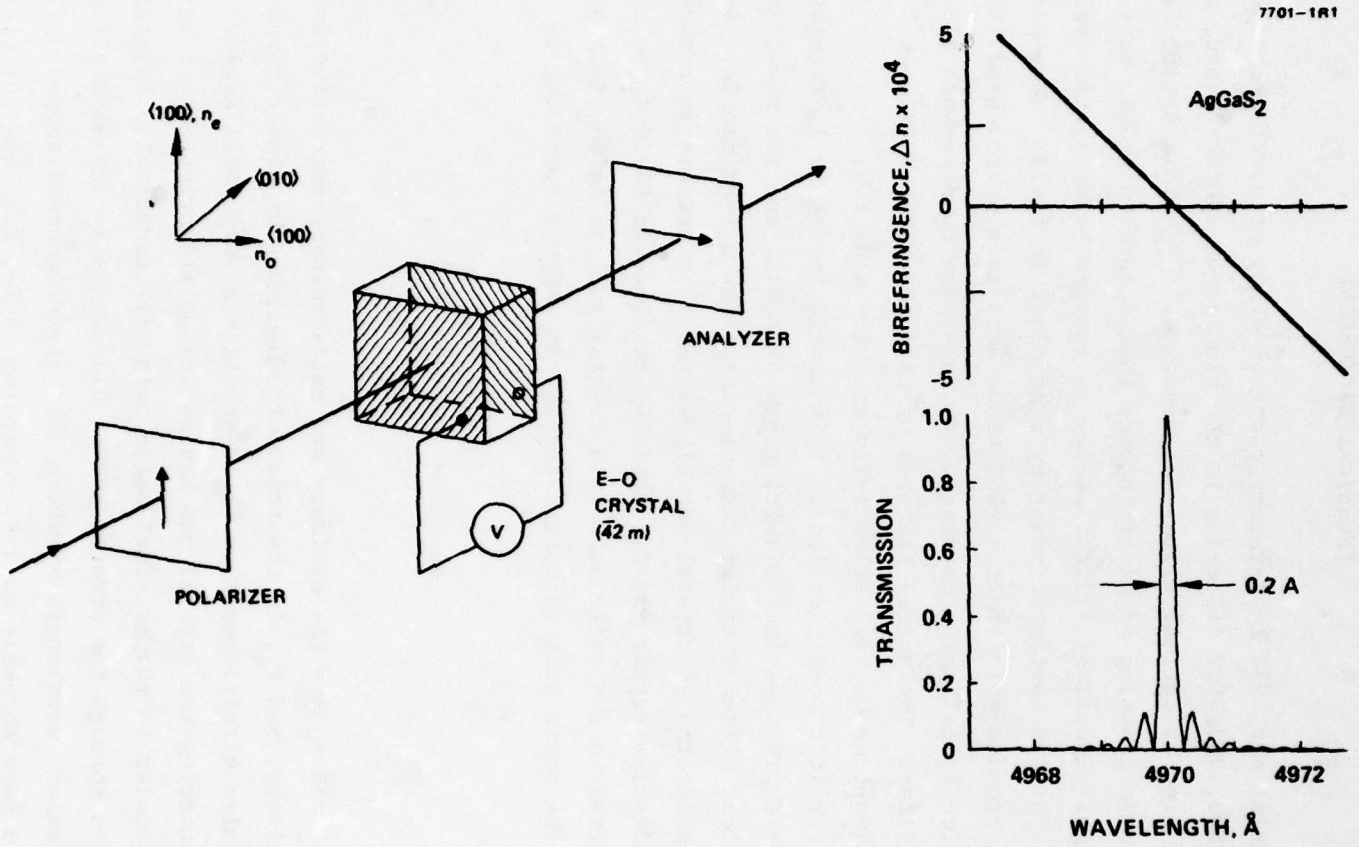

Figure 1. Iso-index coupled-wave electrooptic filter configuration, showing wavelength-dependent birefringence of $AgGaS_2$ and resultant filter transfer characteristic for a 1-cm sample.

changes in the values of the refractive indices depend on $\mathscr{E}_1$ as

$$n_e \to \bar{n} + \frac{1}{2}\,\bar{n}^3 r_{41}\mathscr{E}_1$$

$$n_o \to \bar{n} - \frac{1}{2}\,\bar{n}^3 r_{41}\mathscr{E}_1 \quad , \tag{2.2}$$

where $\bar{n}$ is the average (common) value of n_e and n_o. For this condition, the crystal now has the configuration of a classic Pockels cell.

The transfer characteristic of a lossless filter of length L as a function of wavelength is given by coupled-mode theory:[4]

$$\tau = \frac{(\Gamma L)^2 \sin^2\sqrt{(\Gamma L)^2 + (\Delta kL/2)^2}}{(\Gamma L)^2 + (\Delta kL/2)^2} \quad , \tag{2.3}$$

where

$$\Gamma = \frac{\pi}{\lambda_o}\,\bar{n}^3 r_{41}\mathscr{E}_1 \tag{2.4}$$

and

$$\Delta k = \frac{2\pi}{\lambda}\,(n_e - n_o) \quad . \tag{2.5}$$

An important feature of this filter is its selectivity. This is determined by the rate at which the birefringence, $n_e - n_o$, passes through zero. $AgGaS_2$ exhibits a birefringence[6] with a very abrupt passage through zero at 4970 Å. A crystal having a total interaction length of 1 cm would theoretically have a 3-dB passband of only 0.2 Å and would give full transmission with an applied voltage of a few kilovolts.

An equally important co-feature is the wide FOV characteristic. Theory indicates a limiting FOV of 2π sr with less than a 20% increase in passband over the narrow-field case. The physical reason for the wide FOV is that optical phase matching occurs at all angles at the resonant wavelength.

A more detailed discussion of the theory of operation of the iso-index coupled-wave electrooptic filter appears in Ref. 3, which is reproduced in the appendix.

SECTION 3

EXPERIMENTAL RESULTS

A. SUMMARY

High-resolution measurements of $AgGaS_2$ filter samples, made during this program, confirmed our earlier theoretical predictions. We observed a filter passband of less than 1.0 Å in a sample 3 mm thick and achieved electrooptic control of transmission efficiency up to a maximum of 60% with about 1000 V. These results translate to filter passbands of less than 0.3 Å in a 1-cm sample with comparable voltage requirements and with negligible electric power dissipation. The filter response for off-normal light beams indicated an FOV capability in excess of 60° half-angle (f/0.3) with less than a 20% increase in passband over that of the narrow-field condition. Fine tuning of the pass wavelength by temperature variation has also been observed. A larger tuning range, for matching a particular laser transmitter wavelength, is possible by composition variation.

B. INITIAL OBSERVATIONS

In connection with a proof-of-principle demonstration of the iso-index filter concept, carried out during the previous contract program, transmission measurements in the blue-green spectral region were first made on a highly purified clear sample of (110) $AgGaS_2$ grown and prepared at HRL. The absorptive loss near 4970 Å (the isotropic point of birefringence) was observed to be about 0.10 dB/mm. This was a favorable result since it indicated the practicality of low-loss filter operation at the isotropic point where a full 2π FOV is theoretically possible. Spectrophotometric measurements of the $AgGaS_2$ sample, located between polarizers aligned with its optic axis, showed a narrow "absorption" line at 4970 Å that resulted from elastooptic polarization coupling due to a very small amount of residual strain in the crystal (see Figure 2).

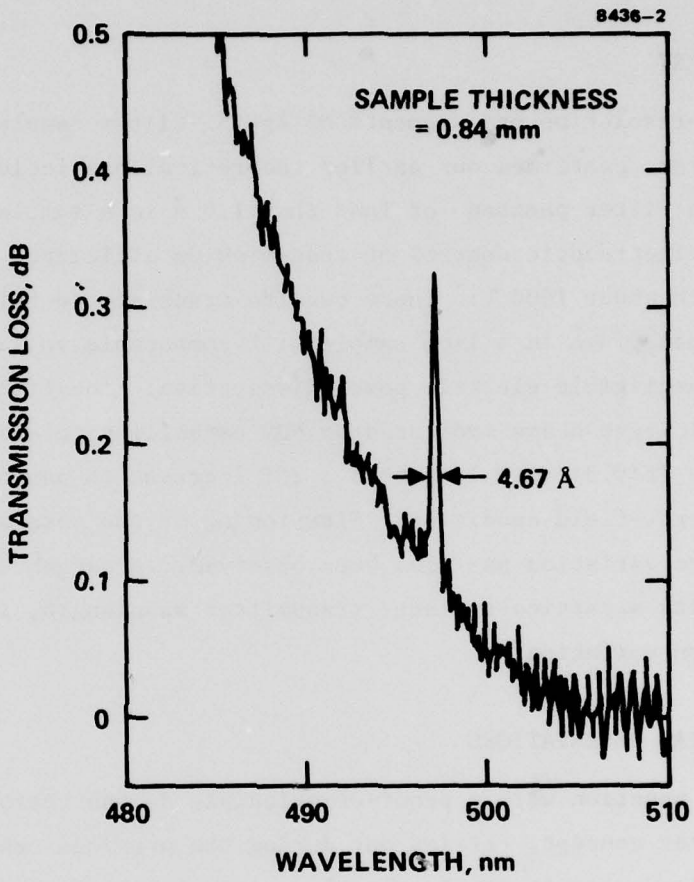

Figure 2.
Room-temperature transmission characteristics of clear $AgGaS_2$ in the blue-green region. Sample thickness = 0.84 mm. Reflective losses not included. Sample between parallel polarizers oriented along optic axis.

C. HIGH-RESOLUTION MEASUREMENTS

The theoretical performance of the iso-index coupled-wave electrooptic filter was verified experimentally using a high-resolution spectrometer. The filter samples consisted of small rectangular blocks of $AgGaS_2$, oriented between crossed polarizers, with light propagating in the <110> direction and electric field applied in the $<1\bar{1}0>$ direction. With white light polarized parallel to the <001> (optic) axis at the input, a narrow band of blue-green light at 4970 Å was, by applying ∿1000 V, coupled into the orthogonal polarization and transmitted by the analyzer. Since no other wavelengths were coupled by the interaction, they were absorbed by the analyzer. Of particular interest was verification of filter action in the 45°-rotated crystal orientation; this orientation permits using a transverse rather than longitudinal electric field. This option allows lower half-wave voltages and lower optical insertion loss. Samples varying in length from 2.5 mm to ∿5.0 mm were tested.

1. Voltage Dependence

Figure 3 illustrates a filter transmission characteristic with and without applied voltage. The curve in Figure 3(a) shows the transmission with no voltage applied. As with all samples tested, a residual transmission was observed in the absence of applied voltage; this was believed due to elastooptic polarization coupling resulting from residual strain in the crystal. The peak transmission of this sample (Figure 3(b)) was ∿60%, obtained with about 1000 V applied across the 0.84-mm thickness. This value of voltage is in close agreement with the predicted value. Figure 4 shows relative transmission of this sample as a function of applied voltage. The theoretical 3-dB bandwidth of this sample (3.2 mm) is 0.63 Å. The larger experimental value of 0.94 Å is believed to be partially due to strain in the crystal and to lack of optimum spectrometer resolution. However, it should be pointed out that no other type of filter of such small size can come anywhere near achieving this narrow a bandwidth.

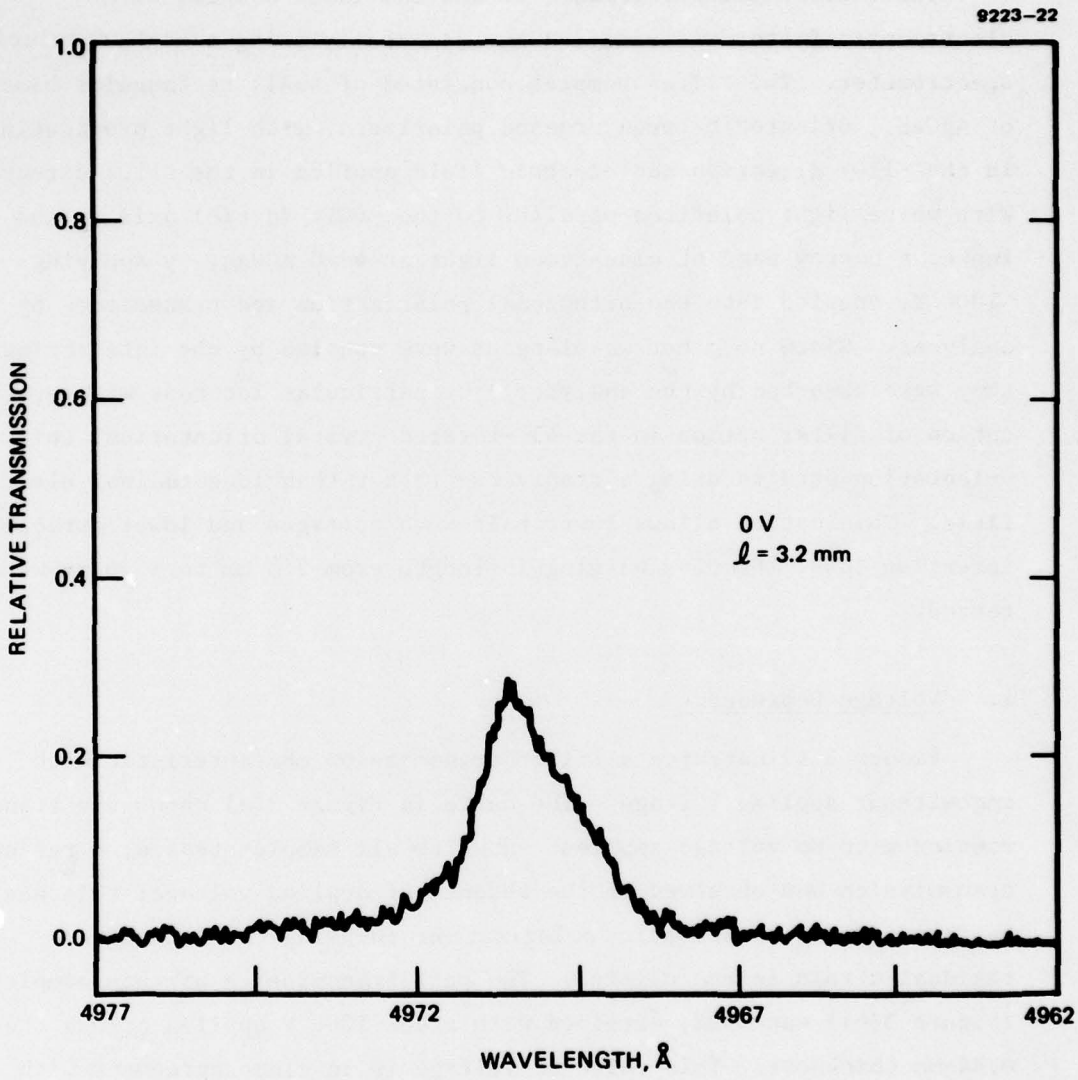

Figure 3(a). Iso-index $AgGaS_2$ filter transmission for a 3.2 mm sample, 0 V applied.

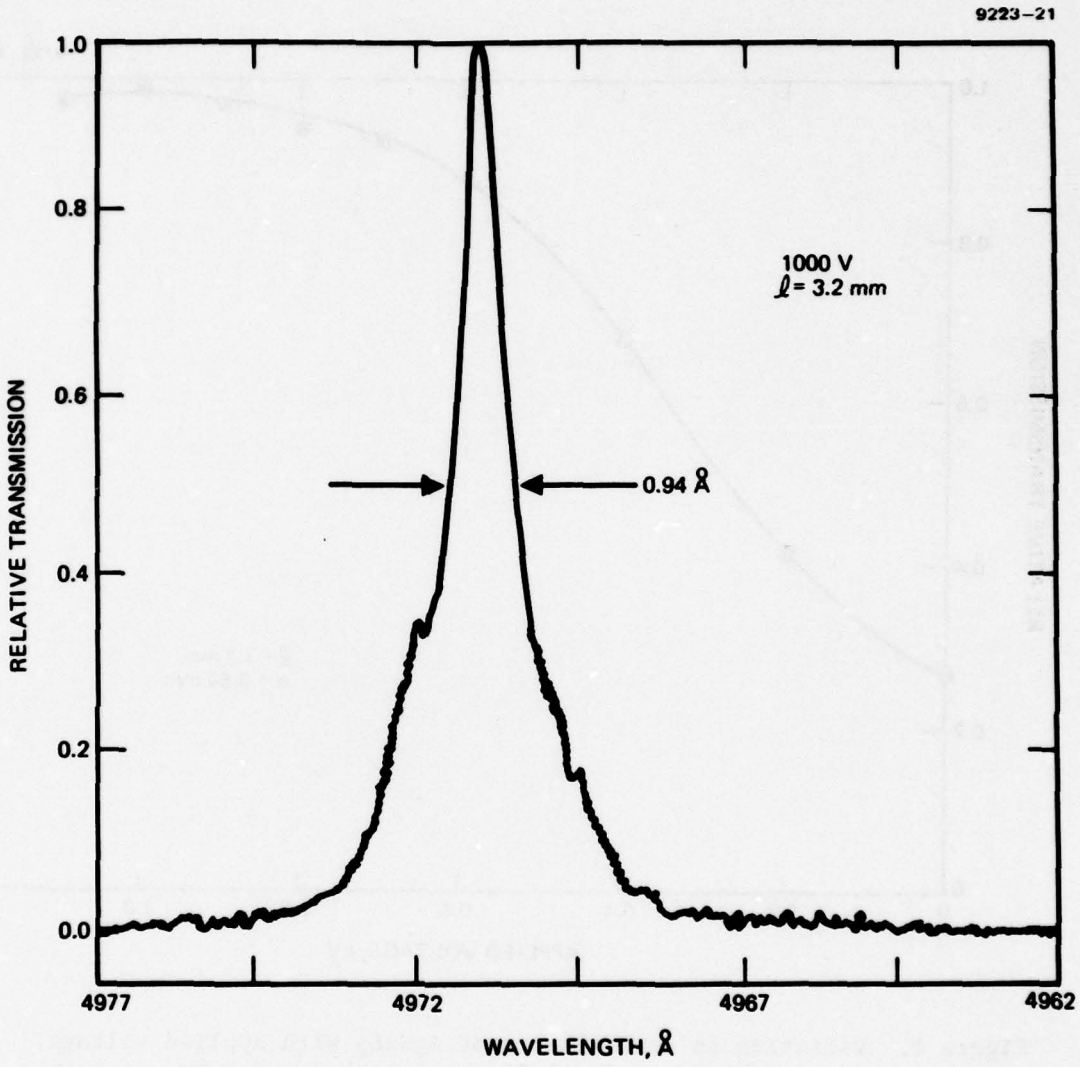

Figure 3(b). Iso-index $AgGaS_2$ filter transmission for a 3.2 mm sample, 1000 V applied.[2]

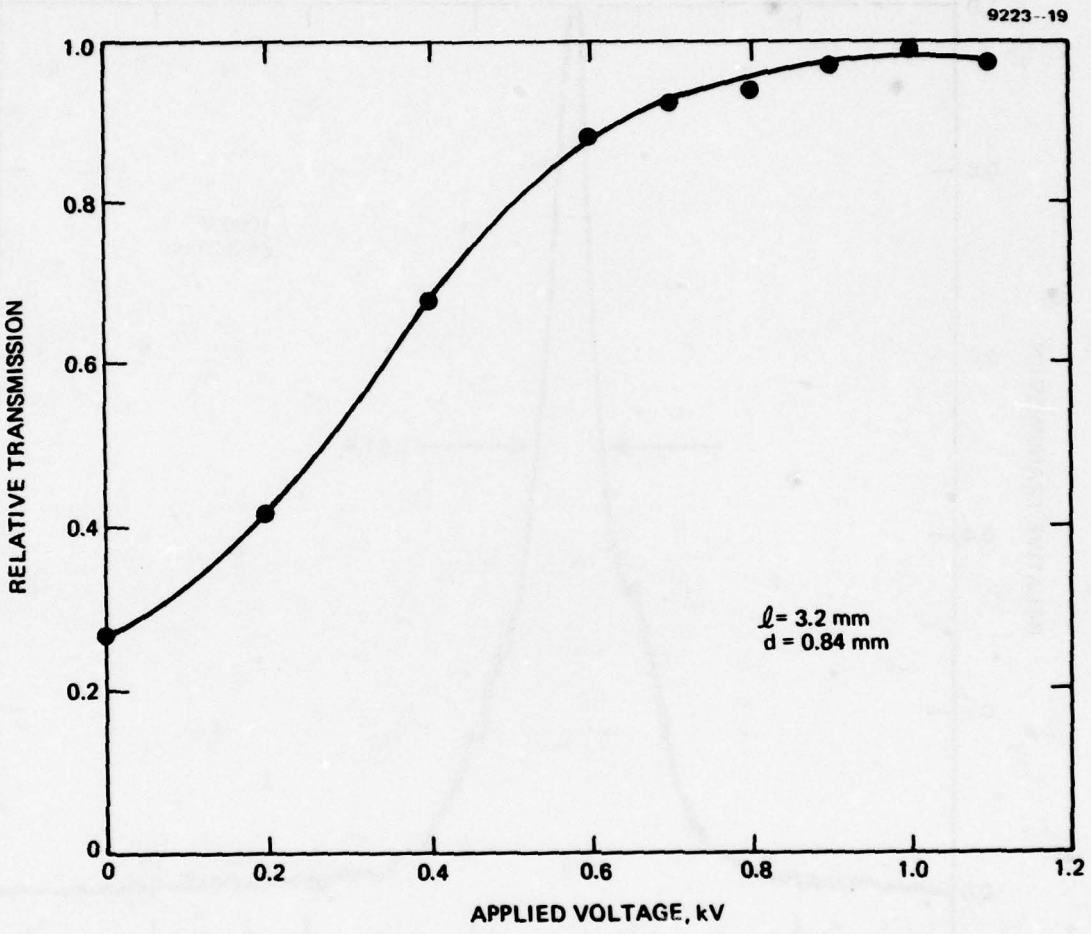

Figure 4. Variation in transmission of $AgGaS_2$ with applied voltage. Sample thickness d = 0.84 mm; length ℓ = 3.2 mm.

2. Field of View

The wide FOV capabilities of this unique type of filter were also verified. Filter passbands were measured for light incident off normal by as much as 60° and compared with those for normal incidence. The results showed that the filter could operate efficiently with an f/0.3 FOV with less than a 20% increase in passband over that of the narrow-field case. By comparison, the state-of-the-art Lyot filter can accommodate at best an f/1 FOV and is substantially bulkier and structurally more complex. Figure 5 illustrates how the passband of the $AgGaS_2$ iso-index filter is affected when the incident cone of light is changed from normal incidence to 60° off normal. The percentage increase in passband observed is considerably less than the theoretical estimate of 15%. Part of the reason for this is, as noted above, the lack of ideal spectrometric resolution, which yields a measured passband somewhat greater than the actual value. Notwithstanding this experimental limitation, the observed results clearly show the wide FOV capabilities of this type of filter.

3. Temperature Tuning

Although the iso-index filter is essentially of fixed wavelength, a modest degree of tuning with temperature was verified. Figure 6 shows the variation of pass wavelength for $AgGaS_2$ with temperature over a range of 10°C above room temperature. The tuning rate is $\sim$0.25 Å/°C. This offers the possibility of fine-tuning, to a limited degree, the filter to track a given transmitter wavelength. We determined that additional, grosser tuning of the passband by compositional variation (e.g., $AgGaS_2$-$CuAlS_2$) to match a desired laser wavelength is also feasible.

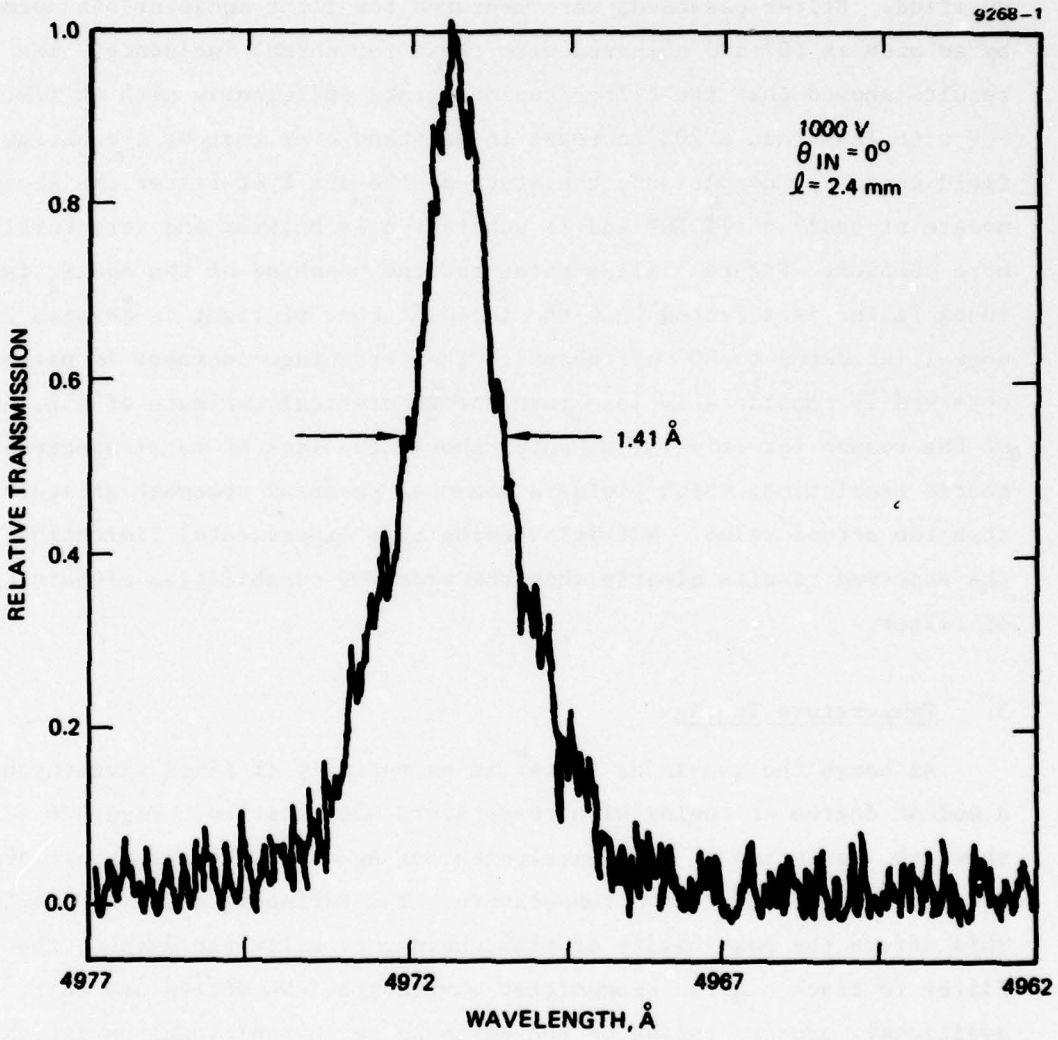

Figure 5(a). Passband of 2.4-mm-long $AgGaS_2$ sample: normal incidence.

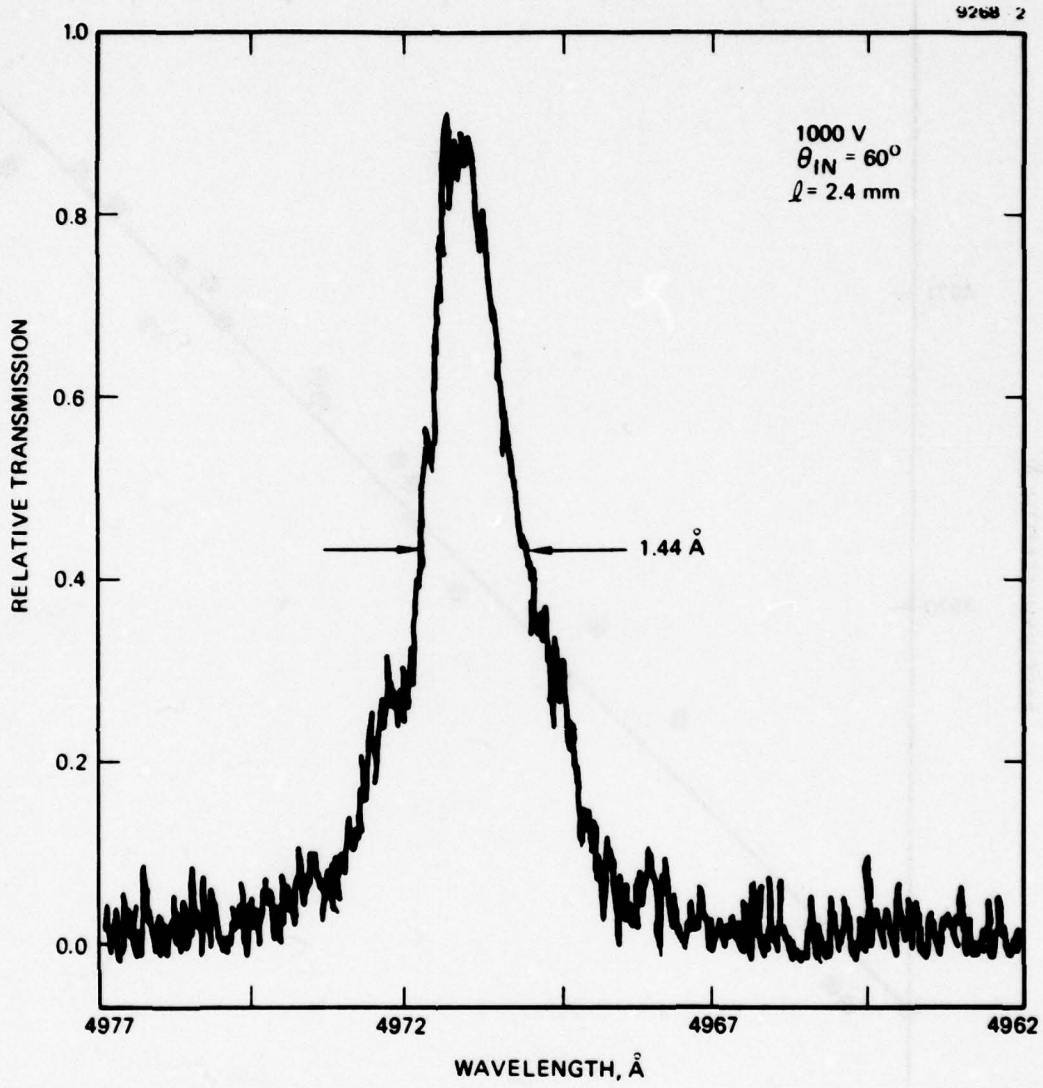

Figure 5(b). Passband of 2.4-mm-long $AgGaS_2$ sample: light incident at 60° off normal.

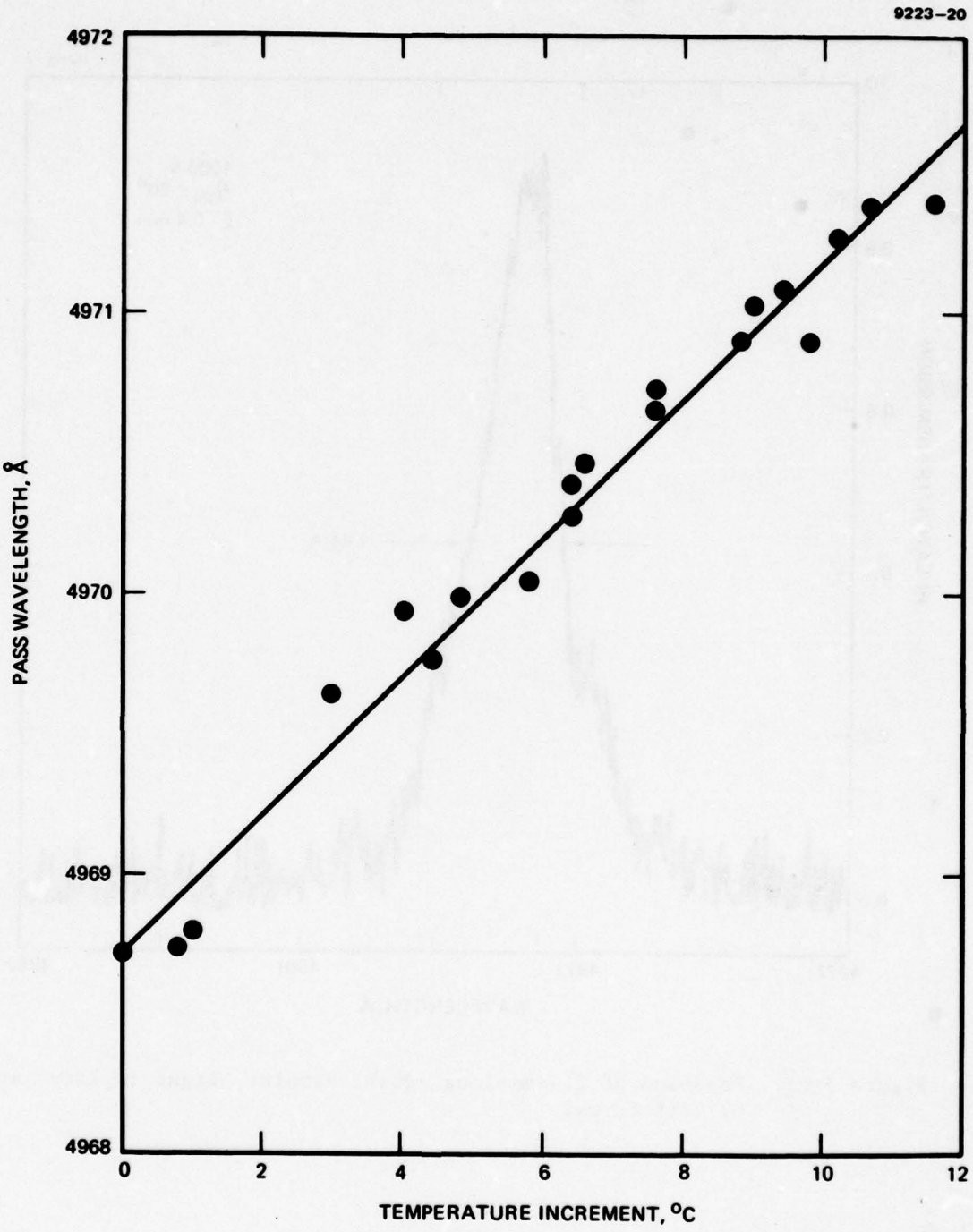

Figure 6. Variation of pass wavelength with temperature in $AgGaS_2$ iso-index filter.

D. WIDE-FOV ANTIREFLECTION (AR) COATINGS

Maximum transmission efficiency of the $AgGaS_2$ iso-index filter can only be realized if Fresnel reflections at the input and output surfaces are minimized. This is particularly important with wide-FOV requirements since reflective losses for s-polarization are especially high at large angles of incidence.

A computer code developed several years ago at HRL allows us to design multilayer AR coatings with specific performance characteristics. In particular, we can design low-reflectance coatings for wide-FOV applications that are polarization independent. Listed in Table 1 are the reflectance values at several angles of incidence for a variety of coating designs. These are AR coatings at 4970 Å on $AgGaS_2$ for unpolarized radiation. These results show that Fresnel losses can be kept below 2% at all angles of operational interest.

Table 1. Reflectance Values of Multilayer AR Coatings on $AgGaS_2$ at 4970 Å for Various Angles of Incidence of Unpolarized Light

Layer 1	Layer 2	Reflection, %		
		0°	22.5°	45°
ThF_4 0.25λ	--	0.83	0.91	2.20
MgF_2 0.25λ	--	3.76	3.85	5.14
CeF_3 0.25λ	--	0.01	0.09	1.45
PbF_2 0.25λ	MgF_2 0.25λ	1.28	1.27	1.41
ZnS 0.25λ	ThF_4 0.25λ	0.48	0.51	1.33
ThF_4 0.351λ	ZnS 0.445λ	0.00	0.69	9.26

6939

SECTION 4

THEORY OF ISO-INDEX CHARACTERISTICS

In this section, we derive a figure of merit for iso-index filters and relate this figure to the optical properties of iso-index materials. From this work, the dependence of filter bandwidth on crystal birefringence and band-edge characteristics is obtained. This knowledge is useful in aiding our selection of new iso-index materials having shorter wavelength crossover points and narrower bandwidths.

A. FIGURE OF MERIT

Iso-index filters derive their narrow bandwidth from the slope $d(\Delta n)/d\lambda$ in the birefringence $\Delta n = n_o - n_e$ at the iso-index point λ_o. From the filter transfer function given in Eq. 2.3, it can be shown that the bandwidth $\delta\lambda_{FWHM}$ for an interaction length L is

$$\frac{\delta\lambda_{FWHM}}{\lambda_o} = \frac{0.8}{L}\left(\frac{d(\Delta n)}{d\lambda}\bigg|_{\lambda=\lambda_o}\right)^{-1} \quad . \tag{3.1}$$

The fractional bandwidth is inversely proportional to the slope of the birefringence and to crystal length. We define the figure of merit $\mathscr{L}'$ of an iso-index filter material as

$$\mathscr{L}' = \delta\lambda_{FWHM} \cdot L \simeq \lambda_o\left(\frac{d(\Delta n)}{d\lambda}\right)^{-1} \quad . \tag{3.2}$$

We choose to normalize this figure to parameters of interest in blue/green programs so that bandwidths can readily be determined from its value. Specifically, a 1-cm-long filter with a 1-Å bandwidth is taken to have a normalized figure of merit $\mathscr{L} = 1$. Thus,

$$\mathscr{L} = \frac{\delta\lambda_{FWHM} \cdot L}{(1\ \text{Å})(1\ \text{cm})} = \frac{\lambda_o}{10^8}\left(\frac{d(\Delta n)}{d\lambda}\right)^{-1} \quad , \tag{3.3}$$

where the slope and wavelength are expressed in angstroms. An $AgGaS_2$ filter operating at 4970 Å exhibits a slope of 1.9×10^{-4} $Å^{-1}$, so its figure of merit is $\mathscr{L} = 0.26$. Thus, a 1-cm-long crystal will have a bandwidth of $\sim$0.26 Å. Alternatively, a 1-Å filter will be realized in a crystal length of $\sim$0.26 cm. For narrowband operation, a small value of $\mathscr{L}$ is desired.

B. ISO-INDEX MODEL

We have adopted a phenomenological model of iso-index materials to relate the slope in birefringence of a given material to the optical properties of its band edge. This model is based on the following observations of known iso-index materials:

- There is a slight shift in the band edge between the ordinary and extraordinary directions of the crystal. This shift is seen in the reflection data of Figure 7.
- The index of refraction away from the band edge is larger for the orientation with the higher energy band edge.
- The iso-index point is well removed from the band edge.

In calculating the iso-index point and its related slope, the last observation allows us to neglect the contribution to the index that arises from absorption. The first two lead to the model schematically shown in Figure 8. The refractive index of the higher energy orientation, indicated by the subscript 1, has the larger index of refraction away from the band edge. The parameters governing the iso-index point and its slope are $\varepsilon_1 - \varepsilon_2$ (recall the dielectric constant $\varepsilon \propto n^2$) and the shift in the band edge.

We now calculate the dependence of the zero-crossing and its related slope on the governing parameters. The dielectric constant of the materials is taken to have two contributions. Near the band edge, a resonant contribution arises from transitions at that wavelength. A constant, nonresonant background term is used to account for all remote

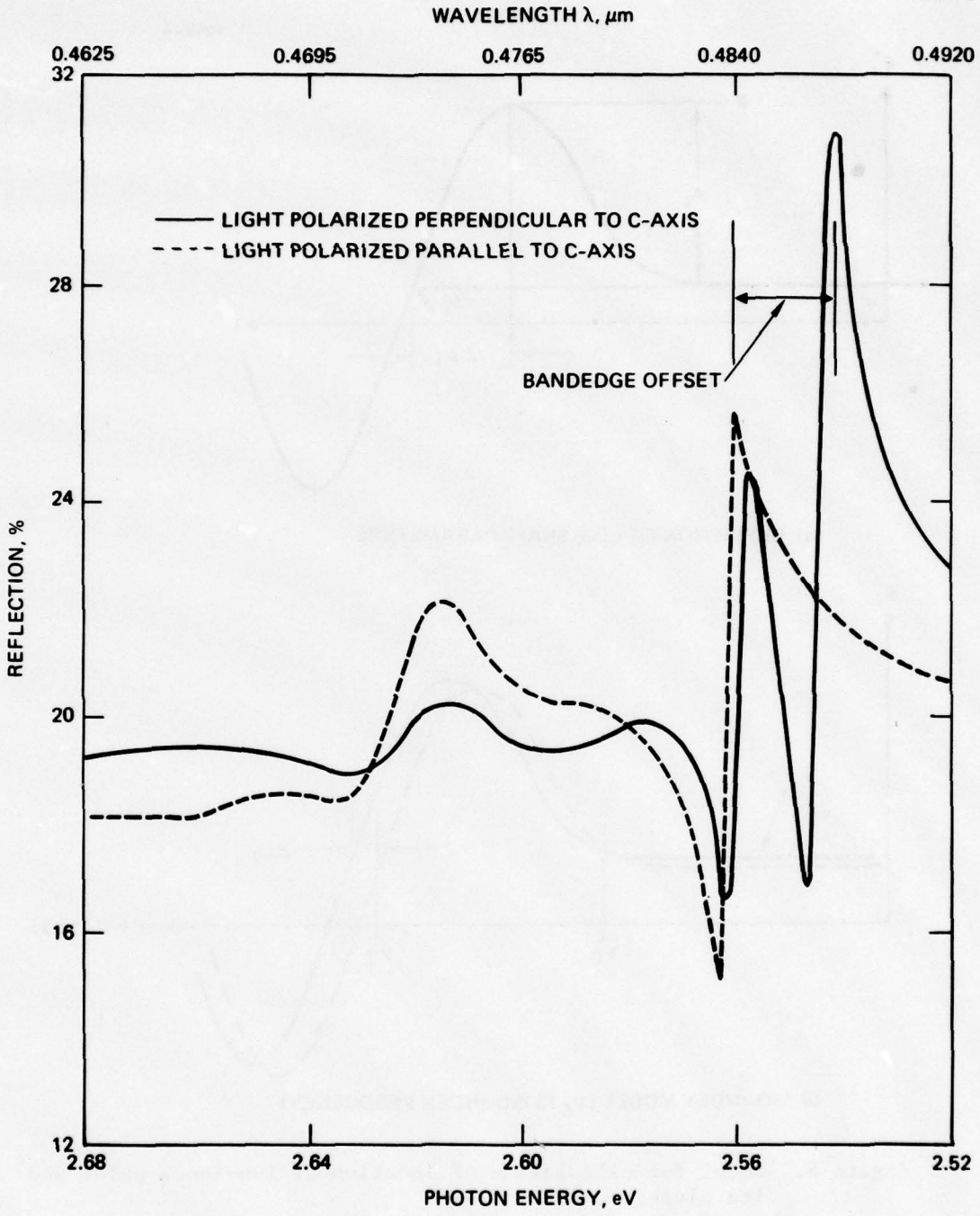

Figure 7. Reflection as a function of wavelength at 77°K for hexagonal, single-crystal cadmium sulfide. (Taken from Ref. 7.)

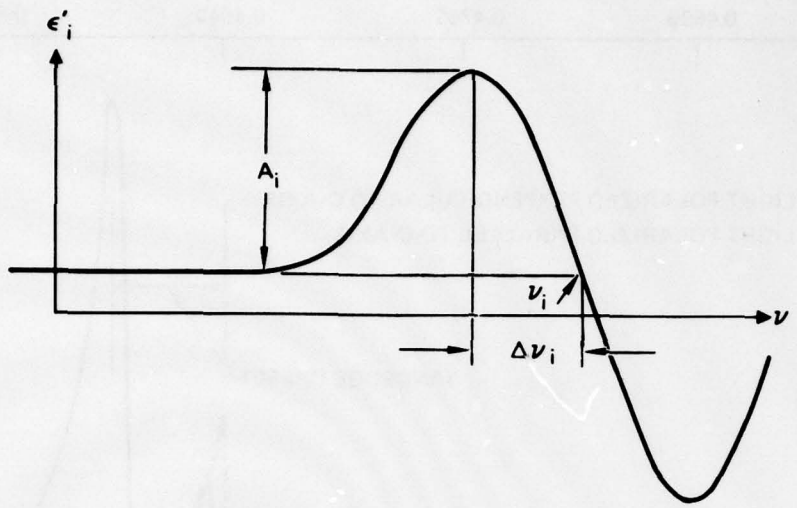

a) DEFINITION OF LINE SHAPE PARAMETERS

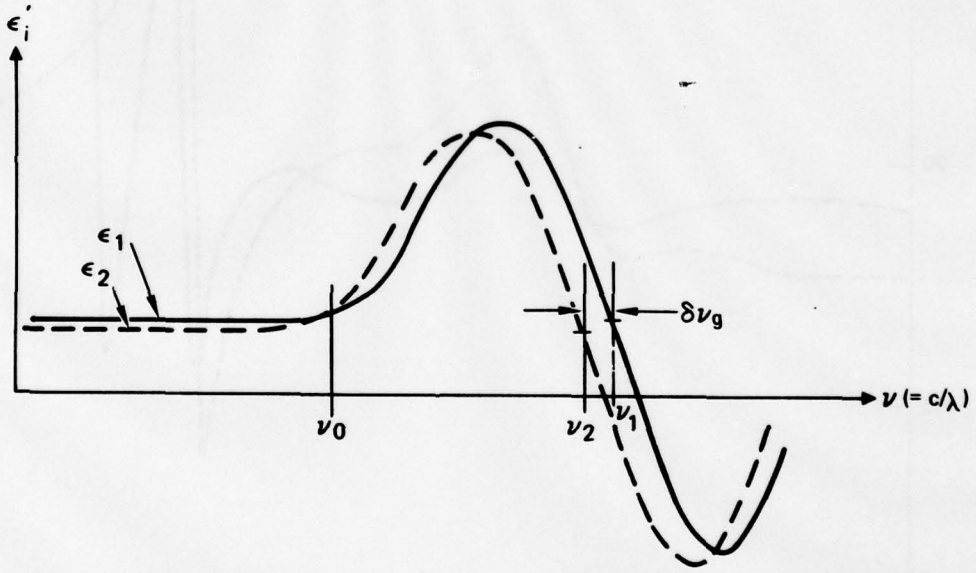

b) ISO-INDEX MODEL (ν_0 IS ISO-INDEX FREQUENCY)

Figure 8. Model for calculation of location of iso-index point and its slope.

transitions as their influence is slowly changing over the range of interest. Thus,

$$\varepsilon_i'(\nu) = \varepsilon_i + \varepsilon_o \sum_j X_{ij}(\nu) \quad , \tag{3.4}$$

where i refers to the ordinary or extraordinary direction, ε_i is the nonresonant contribution, X_{ij} is the susceptibility of the j^{th} resonant transition near the band edge, and $\nu = c/\lambda$. The earlier observation that the iso-index point is well removed from the band edge leads to yet another simplification. The Lorentzian lineshape describing the resonant transitions becomes insensitive to the exact details of the linewidth and falls off as $1/\nu$ in this region. For the j^{th} transition, the susceptibility becomes

$$X_{ij} = \frac{2\Delta\nu_{ij}A_{ij}(\nu_i - \nu)}{(\nu_i - \nu)^2 + \Delta\nu_{ij}^2} \simeq \frac{2\Delta\nu_{ij}A_{ij}}{(\nu_i - \nu)} \quad , \tag{3.5}$$

where the terms are defined in Figure 8. The parameter $\Delta\nu_{ij}A_{ij} \equiv f_{ij}$ is the oscillator strength of the j^{th} transition. Summing Eq. 3.4 over the resonant transitions near ν_i gives

$$\varepsilon_i'(\nu) = \varepsilon_i + 2F_i/(\nu_i - \nu) \quad , \tag{3.6}$$

where $F_i = \varepsilon_o \sum_j f_{ij}$.

We now calculate the dielectric constant difference between the two crystal directions:

$$\Delta\varepsilon = \varepsilon_i' - \varepsilon_2' = \varepsilon_1 - \varepsilon_2 + 2\left[\frac{F_1}{(\nu_1 - \nu)} - \frac{F_2}{(\nu_2 - \nu)}\right] . \tag{3.7}$$

For simplicity, we assume that the oscillator strengths in the two directions are comparable and take $F_1 = F_2 = F$. The success of this model in predicting the zero-crossing and related slopes justifies this

assumption, at least for the II-VI semiconductors and ternary chalcopyrite semiconductors studied. The iso-index point ν_o occurs at the zero of Eq. 3.7, which gives

$$(\bar{\nu}_g - \nu_o)^2 = \frac{2F\delta\nu_g}{\varepsilon_1 - \varepsilon_2} + \left(\frac{\delta\nu_g}{2}\right)^2 \simeq \frac{2F\delta\nu_g}{\varepsilon_1 - \varepsilon_2} \quad , \tag{3.8}$$

where $\bar{\nu}_g = (\nu_1 + \nu_2)/2$ is the average bandgap, and $\delta\nu_g = \nu_1 - \nu_2$ is the difference in bandgaps.

The slope is obtained by differentiating Eq. 3.7:

$$\left.\frac{d(\Delta\varepsilon)}{d\nu}\right|_{\nu=\nu_o} = 2F\left[\frac{1}{(\nu_1 - \nu_o)^2} - \frac{1}{(\nu_2 - \nu_o)^2}\right] = -\frac{4F\delta\nu_g(\bar{\nu}_g - \nu_o)}{\left[(\bar{\nu}_g - \nu_o)^2 - (\delta\nu_g/2)^2\right]^2} \quad . \tag{3.9}$$

Then, by combining Eqs. 3.8 and 3.9 and again neglecting terms of order $(\delta\nu_g)^2$, we get

$$\frac{d(\Delta\varepsilon)}{d\nu} \simeq -\frac{2(\varepsilon_1 - \varepsilon_2)}{(\bar{\nu}_g - \nu_o)} \quad . \tag{3.10}$$

Thus, the slope is merely twice the difference in the nonresonant dielectric constants divided by the separation of the zero-crossing from the mean bandgap.

The slope contained in the figure of merit of Eq. 3.3 is related to that of Eq. 3.10 by

$$\Delta\varepsilon = (n_1' + n_2')(n_1' - n_2') = 2\bar{n}\Delta n \quad .$$

Consequently, Eqs. 3.8 and 3.10 become

$$(\lambda_o - \bar{\lambda}_g) \simeq \left(\frac{F}{c\bar{n}} \cdot \frac{\bar{\lambda}_g^2 \delta\lambda_g}{n_1 - n_2} \right)^{1/2} \tag{3.11}$$

and

$$\frac{d(\Delta n)}{d\lambda} \simeq \frac{2(n_1 - n_2)}{\lambda_o - \bar{\lambda}_g} = \left[\frac{4c\bar{n}}{F} \cdot \frac{(n_1 - n_2)^3}{\bar{\lambda}_g^2 \delta\lambda_g} \right]^{1/2} , \tag{3.12}$$

where again the subscripts o and g refer to the iso-index point and to the bandgap, respectively; $\bar{\lambda}_g$ is the average bandgap; and $\delta\lambda_g$ is the shift in bandgaps.

C. EVALUATION OF ISO-INDEX MATERIALS

In this section, we calculate the zero-crossing and figure of merit of several iso-index materials and compare the values with measured quantities. Numerical values for the band edge shift are obtained from reflection data such as those shown in Figure 7. The crystal birefringence $n_1 - n_2$ away from the band edge is taken from previous measurements such as those in Figure 9.

The measured offset of the iso-index point from the band edge for several II-VI semiconductors and ternary chalcopyrites is shown in Figure 10 along with the calculated offset from Eq. 3.11. The agreement between theory and experiment in Figure 10 is $\sim\pm 15\%$, which we feel is quite adequate considering that there is more than an order of magnitude variation in bandgap splitting $\delta\lambda_g$ and birefringence $n_1 - n_2$ among the materials. The numerical value of the factor $(F/c\bar{n})^{1/2}$ of Eq. 3.11, assumed approximately constant for all materials, was established by

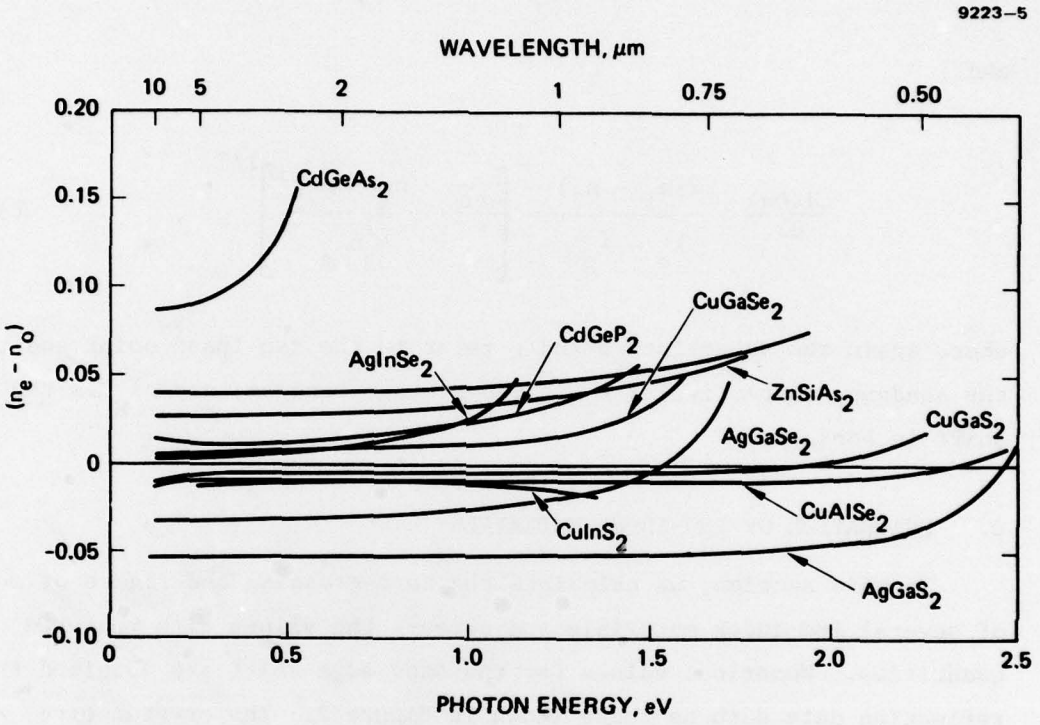

Figure 9. Birefringence of ternary chalcopyrites. (Taken from Ref. 8.)

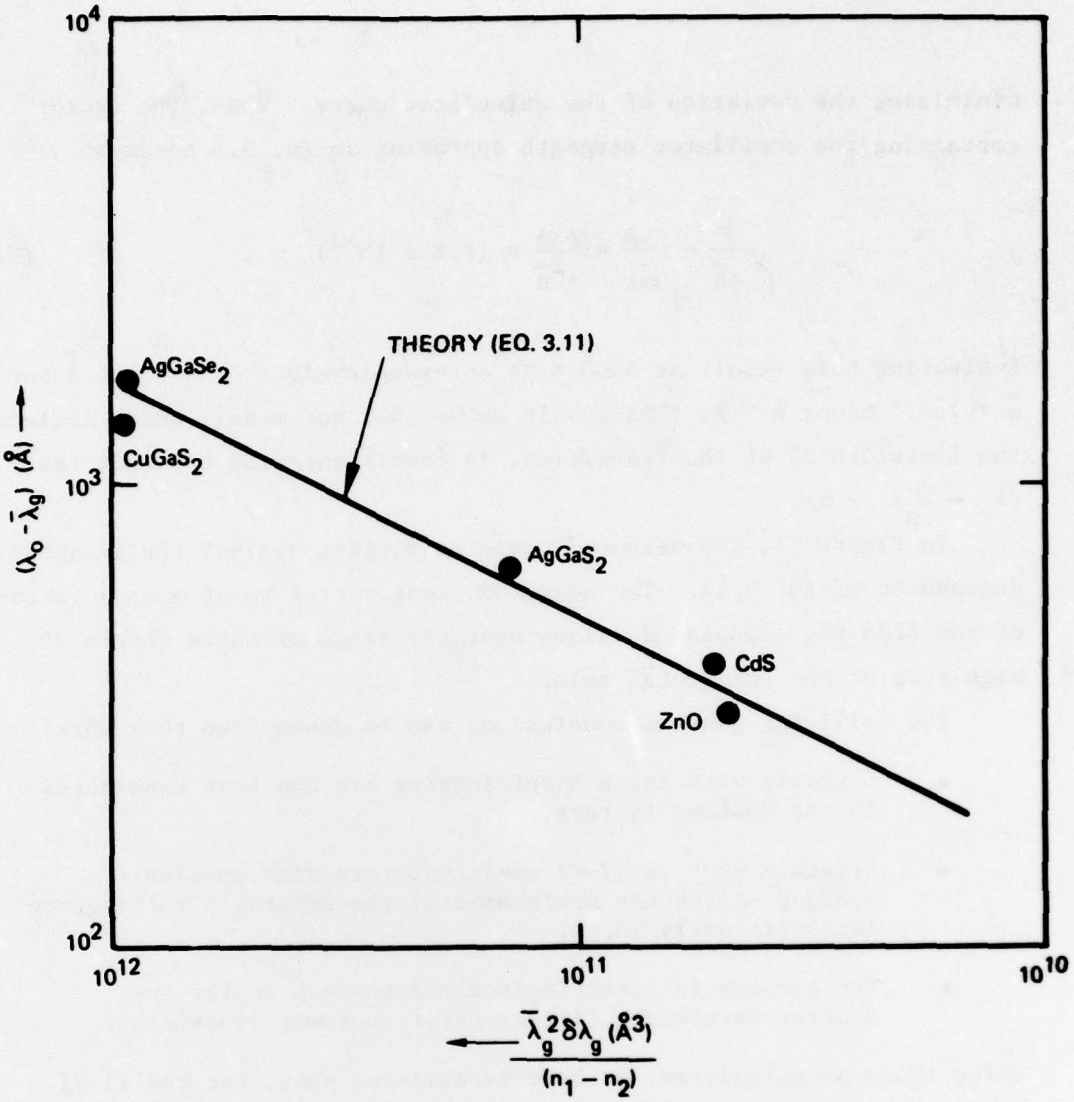

	$\bar{\lambda}_g$ (Å)	$\delta\lambda_g$ (Å)	$n_1 - n_2$	$\lambda_o - \lambda_g$ (Å)
ZnO	3637	48	0.013	323
$AgGaS_2$	4322	422	0.055	648
CdS	4834	38	0.017	411
$CuGaS_2$	4973	240	0.006	1341
$AgGaSe_2$	6429	686	0.030	1607

Figure 10. Measured offset and iso-index point from band edge as function of material parameters.

minimizing the deviation of the calculated curve. Thus, the factor containing the oscillator strength appearing in Eq. 3.6 becomes

$$\frac{F}{c\bar{n}} = \frac{\Delta\nu A}{c\bar{n}} = \frac{\Delta\lambda A}{\lambda^2\bar{n}} = (1.6 \times 10^{-3})^2 \quad . \tag{3.13}$$

Evaluating this result at 5000 Å as an example gives $\Delta\lambda \cdot A \simeq 160$ Å for $\bar{n} \simeq 2.5$. Since $A \simeq 1$, this result shows that our model, which neglects the linewidth $\Delta\lambda$ of the transition, is consistent with the fact that $(\lambda_o - \bar{\lambda}_g) >> \Delta\lambda$.

In Figure 11, the measured slope is plotted against the parametric dependence of Eq. 3.12. The measured slope varies by at most a factor of two from the calculated values over the range of three orders of magnitude of the horizontal axis.

The following general conclusions can be drawn from this work:

- Crystals with large birefringence are the best candidates for narrowband filters.
- Crystals such as II-VI semiconductors with smaller bandgap shifts are preferable if the crystal birefringence is sufficiently large.
- For comparable birefringence and bandgap shift, the shorter wavelength filters offer narrower linewidths.

Using these as guidelines, we have established that, for the II-VI semiconductors, mixed crystals of Cd(Zn)S(O) will provide good iso-index filters in the 4800-Å region while Ag(Cu)Ga(Al)S_2 are good ternary chalcopyrite candidates.

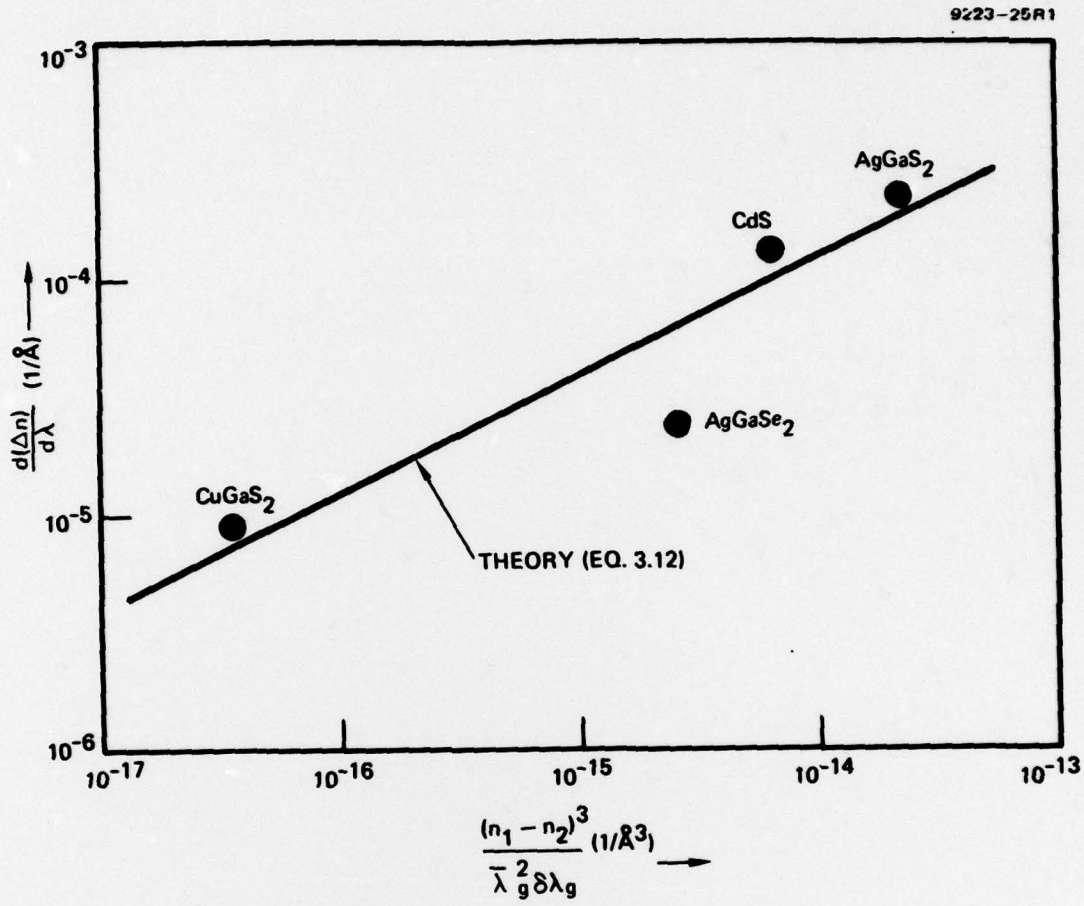

	$\bar{\lambda}_g$ (Å)	$\delta\lambda_g$ (Å)	$n_1 - n_2$	$d(\Delta n)/d\lambda$	$\mathcal{L}$
AgGaS$_2$	4322	422	0.055	1.9×10^{-4}	0.26
CdS	4834	38	0.017	1.2×10^{-4}	0.44
CuGaS$_2$	4973	240	0.006	8.0×10^{-6}	7.9
AgGaSe$_2$	6429	686	0.030	1.9×10^{-5}	4.2

Figure 11. Measured slope at iso-index point as function of material parameters.

SECTION 5

CONCLUSIONS AND RECOMMENDATIONS

This contract study established the feasibility of using $AgGaS_2$ as a narrowband, wide-FOV blue-green filter. Specifically, we demonstrated experimentally (1) a passband capability of 0.9 Å in a 3-mm sample, (2) a transmission efficiency of ∿60% (polarized light) at 1000 V, and (3) an FOV of greater than ±60° (f/0.3) with minimal passband broadening. Follow-on work should extend the technology into a developmental phase to demonstrate a filter with the performance goals listed below:

- Linewidth <0.3 Å
- FOV >±45°
- Peak transmission (unpolarized light) >40%

The following elements are recommended:

- Extend the active area to 1 cm^2 per crystal element
- Improve crystal annealing techniques to remove residual strain
- Employ an alternate coupling mechanism by intentional, directed strain
- Determine out-of-band rejection efficiency.

A. FILTER AREA EXTENSION

Filter crystal elements should be fabricated having active areas of ≥1 cm^2. This represents an extension from current samples having a few square millimeters of useful aperture. The existing samples have for the most part been fabricated in the form of platelets using transverse electric fields of ∿1000 V or less and having apertures of approximately 1 mm x 5 mm. For the larger samples proposed, minimum voltages approaching 4 kV will be required for maximum filter transmittance with interaction thicknesses of 1 cm. The 1-cm thickness will provide the stated linewidth.

B. CRYSTAL STRAIN REMOVAL

The crystal filter samples that were tested gave evidence of residual strain, in greater or lesser degree. This has manifested itself as a residual polarization coupling in the absence of applied voltage. Thus, the filters cannot be completely turned off. Furthermore, we believe that this strain is responsible for the reduced transmission. We should endeavor to improve the techniques of crystal annealing with the aim of removing or minimizing this strain and its effects on filter operating characteristics. Ideally, we would hope to develop crystal filters whose response to applied voltage follows the classic sine-squared law applicable to electrooptic modulators (Pockels cells).

C. ELASTOOPTIC POLARIZATION COUPLING

An alternate method for producing polarization coupling is the application of a controlled, properly directed, strain to the crystal. In $AgGaS_2$ and its isomorphs, a compression along a 45° diagonal in the x-z or y-z plane will generate an x-z or y-z shear strain and thereby cause the same polarization coupling as an applied electric field (longitudinal field) in the y or x direction, respectively. This effect is independent of crystallographic orientation about the optic (z) axis. Thus, the crystallographic orientation of the filter sample is immaterial so long as the optic axis lies in a plane normal to the direction of light propagation. This fact facilitates the mining of useful crystal samples from a boule.

D. OUT-OF-BAND REJECTION

For the characteristic type of $(\sin x/x)^2$ transfer function exhibited by the iso-index filter (see Figure 1 and Eq. 2.3), the theoretical out-of-band transmission is 16% of the total transmission. It would be desirable to carry out high-resolution spectroscopy of filter transmission over a wavelength range of at least 10 times bandwidth and determine the actual out-of-band rejection characteristics of exemplary

filter samples. Apodization techniques to reduce the out-of-band rejection should be investigated. They should include, for example, tailoring the electric field profile along the direction of light propagation. Such techniques have been successfully used in the Hughes electrooptic tunable filter to reduce out-of-band rejection by several orders of magnitude.

REFERENCES

1. J.F. Lotspeich, "Iso-index filter technology," presented at the Strategic Blue/Green Optical Communications Program Review, Office of Naval Research, Arlington, Virginia, May 1979.

2. J.F. Lotspeich, "Iso-index coupled-wave electrooptic filter," presented at the IEEE/OSA Conference on Laser Engineering and Applications, Washington, D.C., May - June 1979.

3. J.F. Lospeich, "Iso-index coupled-wave electrooptic filter," IEEE J. Quantum Electron. QE-15, 904-907, (Sept. 1979).

4. C.H. Henry, "Coupling of electromagnetic waves in CdS," Phys. Rev. 143, 627-633 (Mar. 1966).

5. J.P. Laurenti, K.C. Rustagi, and M. Rouzeyre, "Optical filters using coupled light waves in mixed crystals," Appl. Phys. Lett. 28, 212-213 (Feb. 1976).

6. G.D. Boyd, H. Kasper, and J.H. McFee, "Linear and nonlinear optical properties of $AgGaS_2$, $CuGaS_2$, and $CuInS_2$, and theory of the wedge technique for the measurement of nonlinear coefficients," IEEE J. Quantum Electron. QE-7, 563-573 (Dec. 1971).

7. D.G. Thomas and J.J. Hopfield, "Exciton spectrum of cadmium sulfide," Phys. Rev. 116, 573-582 (Nov. 1, 1959).

8. J.L. Shay and J.H. Wernick, Ternary Chalcopyrite Semiconductors: Growth, Electronic Properties, and Applications, Pergamon Press, New York.

APPENDIX

Iso-Index Coupled-Wave Electrooptic Filter

JAMES F. LOTSPEICH

Abstract—A new optical filter, first demonstrated more than a decade ago and recently extended to other frequencies and materials, is based on the accidental isotropy of refractive indexes that occurs in certain uniaxial semiconductors near the band edge. This paper shows how coupling of light energy can take place between ordinary and extraordinary polarizations at the isotropic point by application of a dc electric field. When placed between crossed polarizers, these materials can thus act as narrow-band filters. The field-of-view characteristics have been analyzed; and it is concluded that this type of filter can, in principle, accommodate a 2π field with less than 20 percent increase in passband over that of the narrow-field condition. It is noted, in particular, that $AgGaS_2$ exhibits the required change of sign of its birefringence at a wavelength of 4970 Å (blue-green), with a rate of change that could provide a passband of only 0.2 Å in a 1 cm sample.

I. Introduction

In 1966 C. H. Henry [1] proposed and demonstrated an optical filter based on the change of sign of the birefringence that occurs near the band edge in certain uniaxial semiconductors [2]. It was shown that coupling of light energy between ordinary and extraordinary polarizations can be effected in CdS at the isotropic point by appropriately applied strain or magnetic field. Thus, when placed between crossed polarizers, the material acts as a narrow-band filter. More recently Laurenti and co-workers [3], [4] have demonstrated a filter tuning capability in mixed crystals of CdS and CdSe. This paper describes how the wave coupling can be effected by an applied dc electric field and proposes the use of $AgGaS_2$ as a highly selective filter material at 4970 Å. The field-of-view characteristics are analyzed; and it is concluded that this type of filter can, in principle, accommodate a 2π field of view with less than 20 percent passband increase over the narrow-field case.

Fig. 1 illustrates two possible configurations of the proposed coupled-wave electrooptic filter. The particular crystal type chosen is one having $\bar{4}2m$ symmetry, for purposes of later illustration and example. As indicated, the filter can be operated with either a longitudinal or a transverse electric field. In the case of $6mm$ hexagonal crystals [1]-[4] only a transverse-field mode of operation is possible. In all cases, the optic axis, denoted by the direction ⟨001⟩, is in the plane normal to the direction of light propagation.

II. Theory of Operation

When an electric field $\mathcal{E}_1$ is applied in the direction as indicated in Fig. 1, a rotation of the optic axis through an angle α in the transverse plane takes place, according to the relationship

$$\tan 2\alpha = \frac{2n_o^2 n_e^2 r_{41} \mathcal{E}_1}{n_o^2 - n_e^2} \tag{1}$$

Manuscript received December 18, 1978; revised March 20, 1979. This research was supported in part by the Office of Naval Research.

The author is with the Hughes Research Laboratories, Malibu, CA 90265.

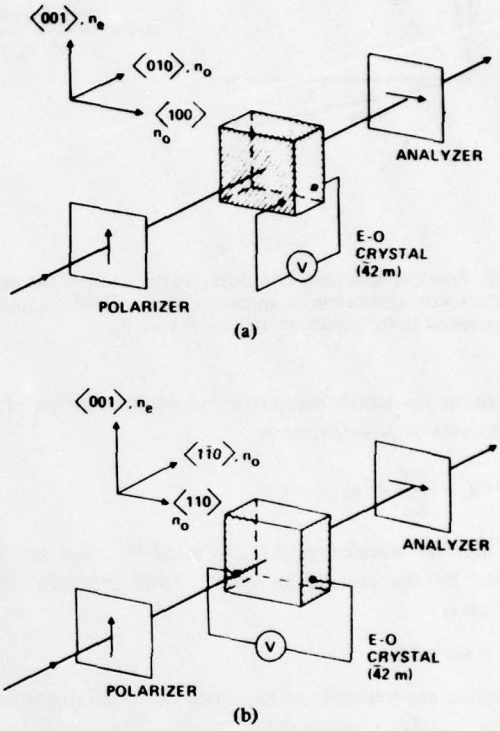

Fig. 1. Coupled-wave electrooptic filter configurations. (a) longitudinal field and (b) transverse field.

where n_o, n_e are the ordinary and extraordinary refractive indexes, respectively, and r_{41} is the relevant electrooptic tensor component. For even mildly birefringent crystals, α is in practice a very small angle. Thus, light entering the crystal having its polarization either parallel or perpendicular to the original optic axis will essentially maintain that direction through the crystal and be blocked by a crossed analyzer. The magnitudes of n_o and n_e remain constant to first order in $\mathcal{E}_1$. If now the birefringence disappears at a particular wavelength λ_0, the right-hand side of (1) becomes infinite with finite field, indicating that α goes abruptly to 45°. The field-induced changes in the values of the refractive indexes, for the new characteristic directions of the principal axes, now depend upon $\mathcal{E}_1$ in first order:

$$n_e \rightarrow \bar{n} + \tfrac{1}{2}\bar{n}^3 r_{41}\mathcal{E}_1$$
$$n_o \rightarrow \bar{n} - \tfrac{1}{2}\bar{n}^3 r_{41}\mathcal{E}_1 \tag{2}$$

where $\bar{n}$ is the average (common) value of n_e and n_o and where we have assumed $n_e > n_o$. These features are illustrated in Fig. 2. At the isotropic point, light of wavelength λ_0, linearly polarized parallel or perpendicular to the original optic axis, will emerge in general elliptically polarized. The crystal now has the configuration of a classic Pockels cell; and for that

0018-9197/79/0900-0904$00.75

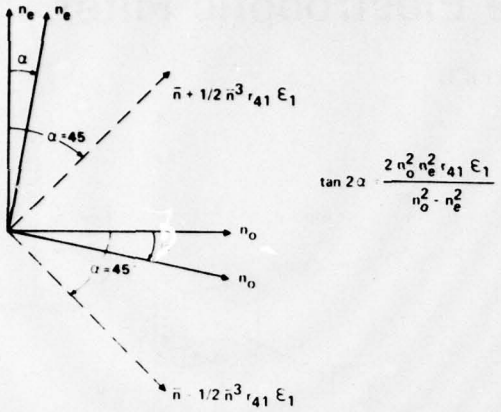

Fig. 2. Principal directions and characteristic values of the index eigenvectors with application of an external field. Dashed lines at $\alpha = 45°$ correspond to the condition of 0 birefringence.

condition for which the relative phase retardation of the two eigenstates of polarization is

$$2\Gamma L = \frac{2\pi L}{\lambda_0} \bar{n}^3 r_{41} \mathcal{E}_1 = \pi, \tag{3}$$

the light at wavelength λ_0 is rotated 90° and totally transmitted by the crossed analyzer. More generally, the transmission is

$$\tau = \sin^2(\Gamma L), \tag{4}$$

a familiar expression from electrooptic modulator theory.

The transfer characteristics of the filter, as a function of wavelength, can readily be derived from coupled-mode theory [1] leading to

$$\tau = \frac{(\Gamma L)^2 \sin^2 \sqrt{(\Gamma L)^2 + \left(\frac{\Delta k L}{2}\right)^2}}{(\Gamma L)^2 + \left(\frac{\Delta k L}{2}\right)^2} \tag{5}$$

where Δk is a phase mismatch term:

$$\Delta k = \frac{2\pi}{\lambda}(n_e - n_o). \tag{6}$$

These expressions are familiar from the theory of nonlinear optics (parametric processes); and (4) is simply a special case of (5) when the phase mismatch is 0.

III. Selectivity

An important feature of this filter is its selectivity. This is determined by the rate of change of the term $\Delta kL/2$ with respect to wavelength. Unlike acoustooptic filters [5] for example, this coupled-wave filter has a selectivity dominated by the rate at which the birefringence, $n_e - n_o$, passes through 0. Laurenti and co-workers [3] demonstrated filter passbands typically 10 to 20 Å in the green for selected samples of CdS_xSe_{1-x} a few millimeters thick. A cursory search of other materials exhibiting this accidental isotropy of refractive indexes revealed that, among the chalcopyrites, $AgGaS_2$ ($\bar{4}2m$ symmetry) exhibits a birefringence [6] with a very abrupt passage through 0 at 4970 Å. Specifically

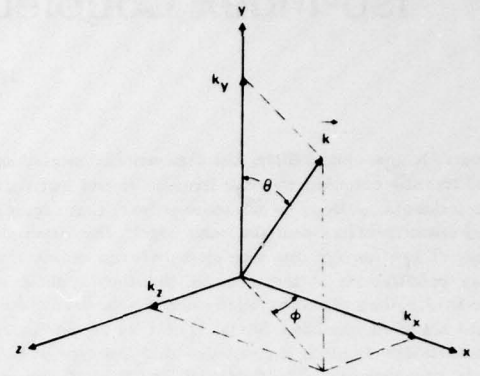

Fig. 3. Coordinate definition for off-axis waves in field-of-view analysis.

$$\frac{d}{d\lambda}(n_e - n_o) = 1.87\ \mu\text{m}^{-1} \text{ at } 4970\ \text{Å},$$

and $\bar{n} = 2.7$. The electrooptic coefficient, according to most recent measurements [7], is

$$r_{41} = 3.2 \times 10^{-12}\ \text{m/V}.$$

These values give a half-wave field-length product

$$(\mathcal{E} \cdot L)_\pi = \frac{\lambda_0}{2\bar{n}^3 r_{41}} = 3.9\ \text{kV}.$$

It can be shown from (5) that, at the half-wave voltage, the half-power point occurs when $\Delta kL = 0.8\ \pi$. Thus, a crystal (or crystals) of $AgGaS_2$ having a total interaction length of 1 cm would have a 3 dB passband of 0.2 Å and would give full transmission with an applied voltage of 3.9 kV in the longitudinal-field configuration and 1.95 kV with transverse field, assuming a $\frac{1}{4}$ cm^2 cross section.

IV. Field of View

An equally important co-feature of this filter is its wide field-of-view characteristic. From a rigorous solution of Maxwell's equations, the generalized coupled-mode equations were derived for non-axial waves. With reference to Fig. 3, we considered a wave vector $\vec{k}$ having polar coordinates θ, ϕ, and Cartesian components k_x, k_z, and k_y. The z-axis was taken to be the optic axis. Two general extreme cases were considered: Case 1 has propagation in the x-y plane ($\phi = 0$ or $k_z = 0$) and Case 2 has propagation in the y-z plane ($\phi = \pi/2$ or $k_x = 0$). For each case, we also considered results from initial polarization mostly along x and mostly along z.

The solutions are as follows.

Case 1: $\phi = 0$ or $k_z = 0$.

$$\Gamma = \frac{\pi \bar{n}^3 r_{41} \mathcal{E}_1}{\lambda}(1 - \delta \tan^2\theta)^{1/2} \tag{7}$$

$$\Delta k_2 = \frac{2\pi}{\lambda}(n_e - n_o)\cos\theta \tag{8}$$

where

$$\bar{n} \equiv \sqrt{n_o n_e} \cong \tfrac{1}{2}(n_o + n_e) \tag{9}$$

$$\delta \equiv \frac{n_e^2 - n_o^2}{n_o^2}. \tag{10}$$

Case 1a: $E_3(0) = 1$.

$$\tau = \left(\frac{\bar{n}}{n_o}\right) \frac{(\Gamma L)^2 (1 - \delta \tan^2 \theta) \sin^2 \sqrt{(\Gamma L)^2 + \left(\frac{\Delta k_2 L}{2}\right)^2}}{(\Gamma L)^2 + \left(\frac{\Delta k_2 L}{2}\right)^2}. \tag{11}$$

Case 1b: $E_1(0) = \cos\theta, E_2(0) = -\sin\theta$.

$$\tau = \left(\frac{\bar{n}}{n_e}\right) \frac{(\Gamma L)^2 \sin^2 \sqrt{(\Gamma L)^2 + \left(\frac{\Delta k_2 L}{2}\right)^2}}{(1 - \delta \tan^2 \theta)\left\{(\Gamma L)^2 + \left(\frac{\Delta k_2 L}{2}\right)^2\right\}}. \tag{12}$$

Case 2: $\phi = \pi/2$ or $k_x = 0$.

$$\Gamma = \frac{\pi \bar{n}^3 r_{41} \mathcal{E}_1}{\lambda} (1 + \delta \sin^2 \theta)^{1/4} \tag{13}$$

$$\Delta k_2 = \frac{2\pi}{\lambda}(n_e' - n_o)\cos\theta$$

$$\cong \frac{2\pi}{\lambda}(n_e - n_o)\cos^3\theta \tag{14}$$

where

$$n_e' = \frac{n_e}{(1 + \delta \sin^2 \theta)^{1/2}}. \tag{15}$$

Case 2a: $E_2(0) = -\sin\theta, E_3(0) = \cos\theta$.

$$\tau = \left(\frac{\bar{n}}{n_o}\right) \frac{(\Gamma L)^2 \sin^2 \sqrt{(\Gamma L)^2 + \left(\frac{\Delta k_2 L}{2}\right)^2}}{(\Gamma L)^2 + \left(\frac{\Delta k_2 L}{2}\right)^2}. \tag{16}$$

Case 2b: $E_1(0) = 1$.

$$\tau = \left(\frac{\bar{n}}{n_e'}\right) \frac{(\Gamma L)^2 \sin^2 \sqrt{(\Gamma L)^2 + \left(\frac{\Delta k_2 L}{2}\right)^2}}{(\Gamma L)^2 + \left(\frac{\Delta k_2 L}{2}\right)^2}. \tag{17}$$

Because of the smallness of δ, the transmission functions in all cases have essentially the form of (5); and they all reduce to (4) at resonance. We note, however, from (8) and (14), that the selectivity is degraded by the factor $\cos\theta$ or $\cos^3\theta$ for beams propagating in the x-y or y-z planes, respectively. For the specific case of $AgGaS_2$, having an index $\bar{n} = 2.7$, the most extreme off-axis angle of propagation is that for which the external incidence angle approaches $\pi/2$; that is

$$\theta_{max} = \sin^{-1}(1/\bar{n}) \approx 22°.$$

This gives

$$\cos\theta_{max} = 0.929,$$

$$\cos^3\theta_{max} = 0.801.$$

Thus, for the two general off-axis cases considered, the passband is increased by only about 7 percent and 20 percent.

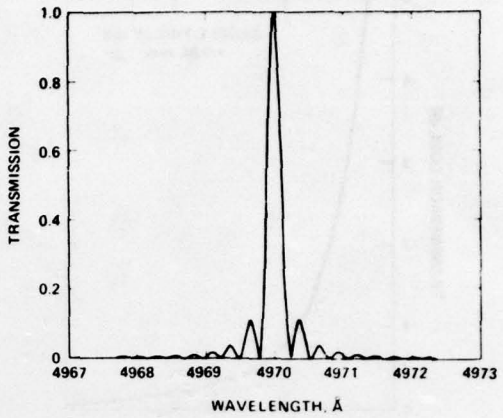

Fig. 4. Filter transfer characteristics of $AgGaS_2$, 10 mm in length, for on-axis rays, with half-wave voltage.

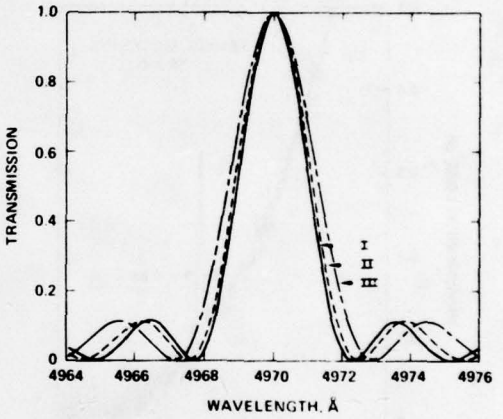

Fig. 5. Filter transfer characteristics of $AgGaS_2$, 1 mm in length. Curve I for on-axis rays, Curve II for extreme off-axis ray in the x-y plane, and Curve III for extreme off-axis ray in the y-z plane.

Sample transmission curves are shown in Figs. 4 and 5. Fig. 4 shows the on-axis case of a $AgGaS_2$ filter, 10 mm in length, having a 3 dB passband of 0.2 Å as predicted from theory. Fig. 5 shows the corresponding case for a crystal thickness of only 1 mm. As expected, the 3 dB passband is increased to 2 Å. Included in Fig. 5 are the two cases of extreme off-axis propagation. The increased passbands in both cases agree quantitatively with predictions.

V. Transmission

A nontrivial limitation of this class of optical filters needs to be pointed out. The zero crossing of birefringence characteristically occurs quite near the band edge. Therefore considerable absorption of the light may result when thick samples are used. This factor has not been included in the above mathematical formulation but may readily be accounted for [1]. Possible means for avoiding or minimizing the band edge problem are currently under investigation.

The situation concerning absorptive loss in $AgGaS_2$ at the isotropic point actually appears to be not a serious one if the material is properly synthesized and annealed. Fig. 6(a) shows room-temperature transmission loss in the blue-green of a highly purified, clear sample of $AgGaS_2$ grown and pre-

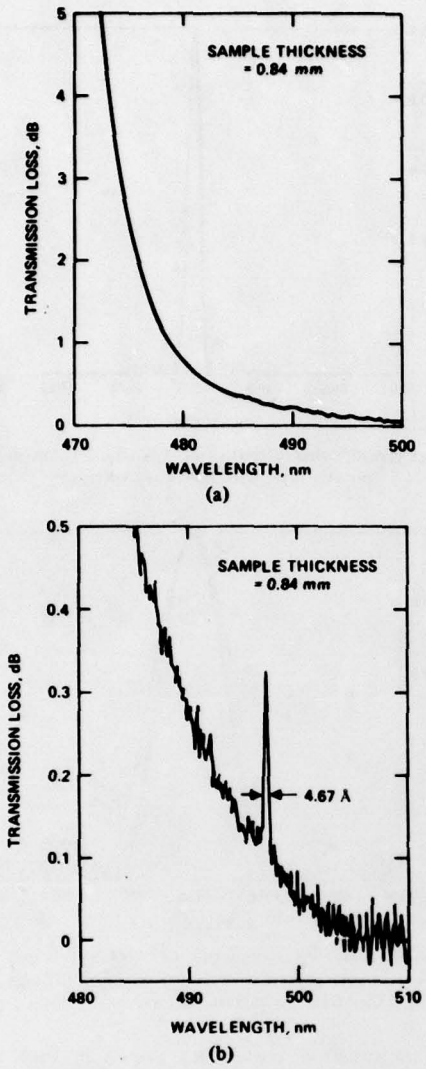

Fig. 6. Room-temperature transmission characteristics of clear $AgGaS_2$ in the blue-green region. Sample thickness = 0.84 mm. Reflective losses not included. (a) Sample alone and (b) sample between parallel polarizers oriented along optic axis.

pared at Hughes Research Laboratories. This is a (110) platelet having a thickness of 0.84 mm. Fresnel reflective losses are not included. The residual absorptive loss near 4970 Å is less than 0.10 dB per mm. Fig. 6(b) shows the transmission characteristics of this same sample between parallel polarizers oriented along the optic axis of the crystal. Note the tenfold increase in spectrophotometer sensitivity. The narrow absorption line at 4970 Å, which is the isotropic point, results from the elastooptic polarization coupling due to a very small amount of residual strain in the crystal. The linewidth is dominated by the spectrophotometer resolution of ~3 Å. Thus the actual material bandwidth is less. A longer interaction length of say, 1 cm, would lead to a filter passband of about 0.2 Å as estimated.

VI. Conclusion

It is apparent from the results discussed above that the iso-index electrooptic coupled-wave filter shows promise of accommodating very wide fields of view while at the same time maintaining a very narrow passband, with proper choice of material and interaction length. Very simply, the physical reason for the wide FOV is that optical phase matching occurs at all angles at the resonant wavelength where the birefringence goes to 0. The necessity for employing well-annealed strain-free crystals is emphasized. Some samples of $AgGaS_2$ not properly annealed were observed to exhibit considerably wider passbands than that shown in Fig. 6(b).

A slight degree of fine tuning of the isotropic point by variations of temperature [1], [3] or of applied strain [3] is expected with $AgGaS_2$, as with CdS and CdSe; and in fact a thermal shift toward longer wavelengths was observed in $AgGaS_2$ on heating, although the temperature sensitivity of tuning has not as yet been measured. Additionally, grosser tuning of the passband by compositional variations, [3], [4] in order to match a desired laser wavelength, should also be feasible [8].

References

[1] C. H. Henry, "Coupling of electromagnetic waves in CdS," *Phys. Rev.*, vol. 143, pp. 627-633, Mar. 1966.
[2] J. J. Hopfield and D. G. Thomas, "Polariton absorption lines," *Phys. Rev. Lett.*, vol. 15, pp. 22-25, July 1965.
[3] J. P. Laurenti, K. C. Rustagi, and M. Rouzeyre, "Optical filters using coupled light waves in mixed crystals," *Appl. Phys. Lett.*, vol. 28, pp. 212-213, Feb. 1976.
[4] J. P. Laurenti, K. Rustagi, M. Rouzeyre, H. Rufer, and W. Ruppel, "Graded-composition semiconductors as tunable narrow-band optical filters," *J. Appl. Phys.*, vol. 48, pp. 203-204, Jan. 1977.
[5] S. E. Harris and R. W. Wallace, "Acousto-optic tunable filter," *J. Opt. Soc. Amer.*, vol. 59, pp. 744-747, June 1969.
[6] G. D. Boyd, H. Kasper, and J. H. McFee, "Linear and nonlinear optical properties of $AgGaS_2$, $CuGaS_2$, and $CuInS_2$, and theory of the wedge technique for the measurement of nonlinear coefficients," *IEEE J. Quantum Electron.*, vol. QE-7, pp. 563-573, Dec. 1971.
[7] T. K. Plant, Hughes Res. Lab., Malibu, CA, private communication.
[8] A. L. Gentile, Hughes Res. Lab., Malibu, CA, private communication.